Dynamically tuned shroud for gun barrel vibration attenuation

Andrew G. Littlefield, Eric L. Kathe, Robert Durocher

US Army, TACOM-ARDEC, Benét Laboratories, Watervliet Arsenal, Watervliet, NY 12189

ABSTRACT

Modern tank guns, such as the one on the Abrams, are stabilized to allow fire on the move while traversing uneven terrain. The current barrel is short enough that treating as a rigid beam allows engagement of another tank at ranges of over a kilometer. However, as the length of the tube is extended, to meet required muzzle exit velocities, the terrain induced vibrations lead to increased muzzle pointing errors. A method to reduce these vibrations is to use the forward thermal shroud as part of a mass tuned damper. In this case the system under study is an extended length version of the gun currently fielded. This extended length increases its susceptibility to terrain-induced vibrations. The forward thermal shroud has been shortened and additional mass has been added onto its forward collar. This collar is then supported by springs, which are preloaded so that they stay in contact through the full range of the shroud's movement. Varying the stiffness of these springs allows for tuning of the absorber. Different types of springs and attachments have been tried. The current version uses leaf springs and a wedge collar. This system has been modeled and experiments conducted to validate the model.

Keywords: vibrations, vibration absorber, cannons, gun barrel, passive, accuracy, dynamics

1. INTRODUCTION

Vibration of the gun barrel leads to dispersion in the shot patterns. The wider the dispersion the more rounds required to affect the desired damage on the enemy. An intuitive way to reduce this shot dispersion is to reduce the vibrations of the barrel. The end of the barrel is the anti-node for all vibration modes and its vibrations have the greatest affect on shot dispersion, so it is the obvious location to attempt to dampen the vibrations. This work focuses on doing just that.

The system under study is the 120mm M256E1 cannon. This is an extended length version of the M256 cannon currently fielded on the M1 Abrams. The M256E1 is 6.6 m in length compared to 5.3 m for the M256. This increase in length is necessary to achieve the required exit velocities. This increase in length though, increases the barrel's receptance to environmentally induced vibration. (Receptance is the ratio of vibration amplitude to force as a function of frequency[1].) While launch induced vibrations are certainly important, trying to structurally control the barrel during the available time window, typically less than eight milliseconds, is a daunting task beyond the scope of the present work. So we will focus solely on environmentally induced vibrations.

The absorber being considered is a spring collar that mounts onto the forward end of the gun's front thermal shroud. The primary function of the shroud is to prevent thermal gradients within the barrel that would otherwise cause unacceptable distortions (e.g., direct sunlight heating one side of the barrel). The back of the forward shroud is affixed to the bore evacuator using a compression collar that enables a pivoting action; this prevents thermal distortions in the shroud from being transmitted to the barrel. By connecting to the shroud we are able to use the mass of the shroud as part of the mass of the absorber. The absorber is tuned by adjusting the mass and springs in the spring collar. By using a slightly shortened shroud we are able to stay inside the space originally set aside for the thermal shroud and have minimal impact on system configuration. This approach was termed the dynamically tuned shroud (DTS)[2].

Originally coil springs were used. Then these were replaced with leaf springs with adjustment screws and then leaf springs with a wedge collar. We will look at why these changes were made and how the current configuration was determined. Some of the problems with the current design will also be mentioned.

Figure 1 Original dynamically tuned shroud (DTS) approach

The barrel is modeled in MATLAB® using a finite element approach[3]. The Euler-Bernoulli finite element technique is used to generate second order equations of motion of the barrel as a non-uniform beam. These are then converted to the first-order state space domain and transformed into the frequency domain. Predictions for the mode shapes and resonant frequencies are generated. After completing the model, it is verified by performing modal impact testing on the barrel. These results are then used to fine-tune the model.

Testing of the barrel with different vibration absorbers is then conducted. Three different versions are used, the differences being the stiffness of the springs connecting the absorber to the barrel. These results will be compared to predictions of the MATLAB® model.

2. HISTORY

The original concept for the DTS used compression springs mounted on the end of the thermal shroud. The spring collar itself had little added mass. To increase the mass additional weights were added to the collar. To change the stiffness of the absorber the preload of the springs could be changed. By altering these two parameters the natural frequency of the DTS could be tuned. A picture of this approach can be seen in Figure 1[4].

This approach was tested on a 120 mm XM291 cannon on the bump course at Aberdeen Proving Grounds, Maryland and showed a 24% and 9% RMS improvement in vertical and horizontal bending, respectively[5]. No live fire testing was conducted though as there were doubts about the robustness of the hardware. The shroud being used had already been blown off one gun and the attachment of the spring collar was via ordinary screws.

The effectiveness of this absorber spawned other efforts. A medium caliber absorber[6] was designed and shown to be effective[7]. However a more robust version of the large caliber DTS was desired. The goal was to come up with a

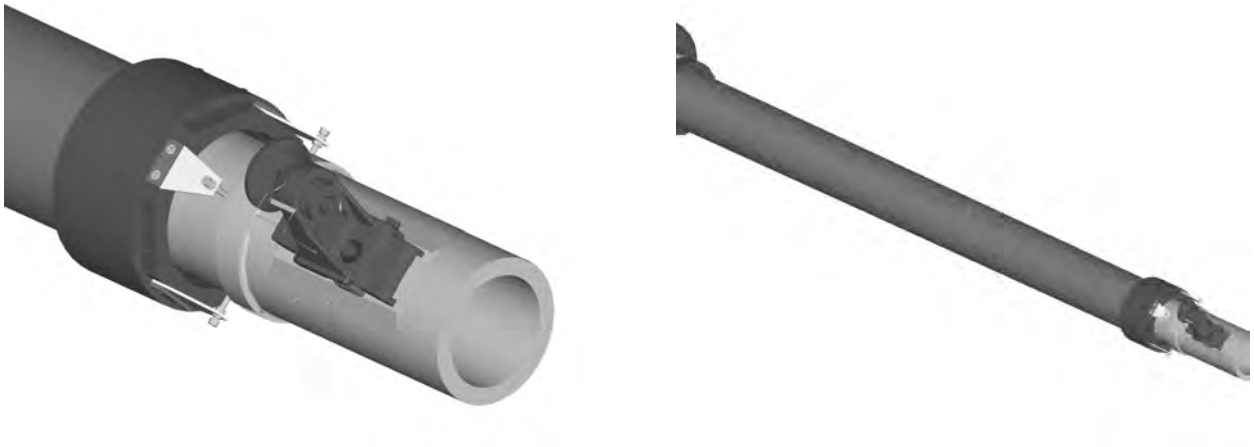

Figure 2 Second DTS concept

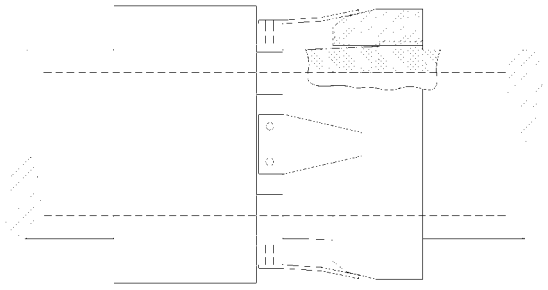

Figure 3 Current DTS concept

weaponized version that could be tested in the field.

During testing of the original DTS it was found that adding weights to the end of the shroud increased performance. So in the new design the spring collar was designed to have a substantial mass, 15.8 kg. The profile of the compression springs was found to be high enough that they may interfere with the optics of the muzzle reference system (MRS). Also there were questions about their reliability under use conditions. For these reasons it was decided to use leaf springs. These springs would be rigidly attached to the collar at one end and be supported by an adjusting screw at the other end. By turning this screw the preload could be adjusted. In order to keep the entire assembly out of the line of sight of the MRS optics it was sized so that the absorber could move 3mm in any direction. Three springs of different stiffness were selected so that they would remain in contact with the tube throughout this range of motion. All parts of the assembly were designed to withstand firing loads. A picture of this approach can be seen in Figure 2. Although four springs are visible in the picture the collar was made to accommodate up to eight springs.

This approach was supposed to be tested in house and then sent to Aberdeen Proving Grounds for testing. The testing was to include both firing and non-firing tests on the bump course. However problems arose during the in house testing. The screws meant to preload the leaf springs did not ride smoothly on the surface of the tube and caused the spring to twist as it was loaded. Also they tended to kick out and get stuck if the absorber was hit with enough mass to cause it to bottom. This type of loading would definitely be present during firing, so it was decided that a redesign was needed.

The third and current version of the DTS still uses the leaf springs but the adjusting screws are gone. Instead a wedge ring is now mounted on the threads used for forward attachment of the standard thermal shroud. As it is screwed on the wedge engages the springs and forces them out to a preset distance. This distance is set so the absorber still has its full 3 mm range of motion in any direction. The springs are allowed to ride on the wedge ring so there is no sticking or twisting as was found in the previous design. The apparent stiffness of the spring can be changed turning the wedge ring in or out. The whole DTS still fits in the space of the normal thermal shroud and does not interfere with MRS optics. This is the design modeled and tested in the rest of the paper. It can be seen in Figure 3. Originally it was to be tested at Aberdeen in place of the second concept but the additional time required to design and fabricate the new wedge ring prevented this from happening.

3. MATLAB® MODEL

A finite element model of the barrel was created in MATLAB®. Euler-Bernoulli beam approximations and Hermite-cubic interpolation functions are used to form the mass and stiffness matrices for the undamped second order equations of motion by approximating the barrel, a continuous non-uniform beam, as a series of discrete elements. Continuity of lateral displacement and slope are imposed at the element boundaries. When assembled these elements closely approximate the dynamics of the barrel[4].

The geometry of the barrel is entered in 1 mm increments and any non-circular cross sections are smeared together to become circular. The DTS hardware was added to the model as non-

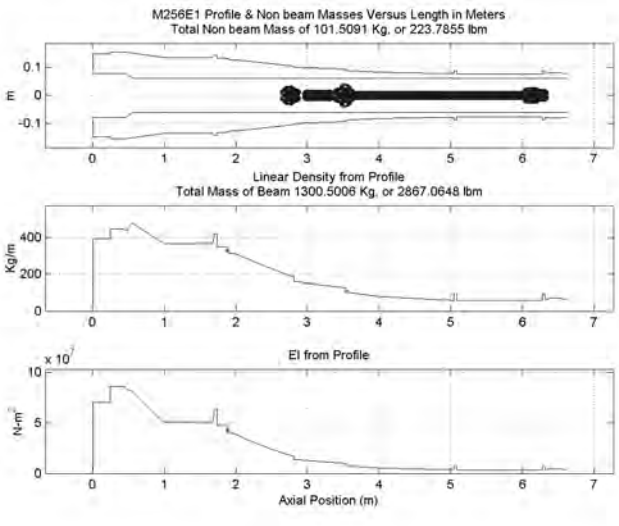

Figure 4 Barrel geometry

beam lumped masses. The mass of each part was distributed over its length so that the center of gravity for each item was in the correct space. For this first version the absorber was treated as another lumped mass with no springs. The mass of the beam is calculated by adding the mass of each of both the beam and non-beam slices. The model's version of tube can be seen in Figure 4.

After the geometry has been entered the barrel is automatically broken into a user defined number of elements. Nodes are forced to exist at both ends of the barrel and anyplace where constraints are specified. In this case nodes were added at the location of the front and rear supports, the location where the hammer impulse would be delivered and where the absorber will interact with the barrel. Even though the absorber wasn't in this version, this was done to keep changes between versions to a minimum.

Figure 5 Test setup

Ideally we would like to hang the tube by soft springs. Originally this was to be accomplished by striking the tube sideways with the supports acting as a pendulum. A sling suspended from a gantry was used near the breech end and multiple wraps of bungee cord suspended from a jib crane were used in the front. This setup can be seen in Figure 5. In this configuration, so long as the supports were long enough, very little energy would go into raising the barrel for small sideways displacements. Thus the supports would approximate very soft springs. We were able to generate data for the non-absorber barrel in this configuration.

However when it came time to test the barrel with the vibration absorber installed we were unable to get any useful data. Testing in this configuration required the use of multiple springs on this absorber. We found that we were not able to introduce enough energy into the system to properly excite the absorber. To overcome this problem we changed to testing vertically, which required us to find the stiffness of the supports. This was found by suspending known weights from them and measuring the displacement. The effect of the less than soft rear support was minimized by placing it at the anti-node of the first mode. The location of the anti-node was found by running the model with no constraints. This location also turned out to be close to the anti-node for the second mode.

Rayleigh proportional damping is used in the model. Initially values from a previous report using this software for analyzing an XM291 gun barrel[8] were used. After performing an experimental modal analysis on the barrel, experimentally found values were used and the model was rerun. Only minor differences in the resonant frequencies were found.

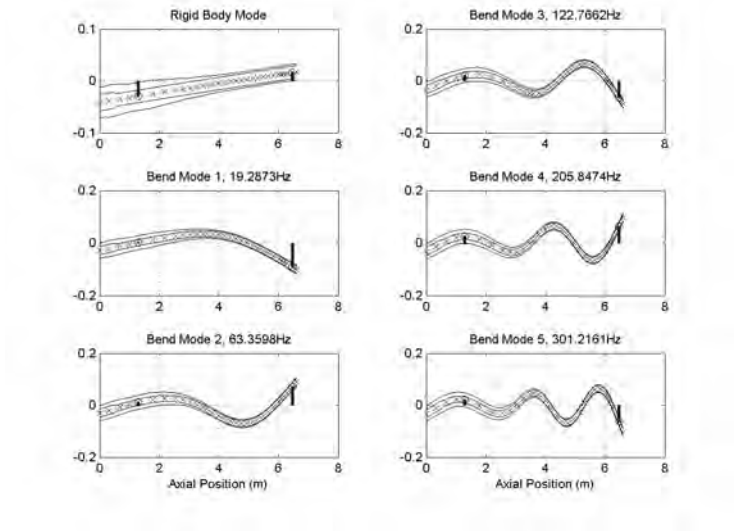

Figure 6 Damped mode shapes and natural frequencies of the base system

After the required data was entered the model was run and output generated. The software generates undamped and damped mode shapes and natural frequencies, a pole zero plot of the eigenvalues, time response of the muzzle to a breech impulse, and a bode plot of the muzzle response, plus additional plots about the quality of the FEA analysis. In this case we are interested in the damped mode shapes and natural frequencies. These can be found in Figure 6.

4. MODAL IMPACT TESTING

After completion of the MATLAB® model, an experimental modal analysis was performed to validate the model. The barrel was hung from a sling at the breech and bungee cord at the muzzle.

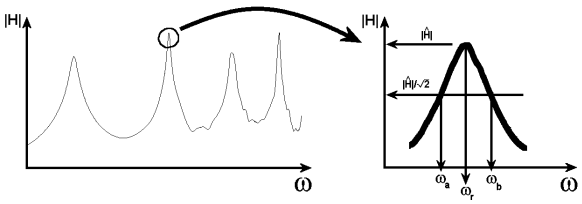

Figure 7. Peak amplitude method

The idea was to simulate a free-free condition. As mentioned above the rear support was placed at the anti-node of the first mode so as to limit its influence. Since the supports were explicitly contained in the model this was deemed satisfactory.

The goal of the modal analysis was to generate a frequency response plot between a force at the breech and the response of the muzzle. For this study an impact was used as the force and the acceleration of the muzzle was the response. An HP 3566A PC Spectrum / Network Analyzer was used to calculate the frequency response. A PCB Impact Hammer with a super soft tip delivered the impact. The 6 dB roll off point of the tip was found to be 200 Hz. A PCB ICP Accelerometer measured the response. The ICP power supply and signal conditioning for both of these was provided by a PCB 12 Channel Rack Mounted Power Unit with a variable gain of 0 to 100 per channel. This can be seen in Figure 5.

The HP 3566A was setup with a bandwidth of 800 Hz, 3200 frequency lines and force / exponential windowing. Uniform averaging was performed with a total of 10 averages being used per run. The gain was set to provide good signal strength. After each impact the data was checked for double hits and overloading of the accelerometer.

The Peak Amplitude Method[1] was used to extract the necessary modal parameters from this data. To determine the damping ratio of a peak, equations (1) and (2) were used.

$$\zeta = \tfrac{1}{2}\eta \tag{1}$$

$$\eta = \frac{1}{2}\frac{\omega_a^2 - \omega_b^2}{\omega_r^2} \tag{2}$$

Where ζ is the viscous damping ratio, η the structural damping loss factor, ω_r is the natural frequency of the peak, and ω_a and ω_b are the half power points. These quantities can be seen in Figure 7.

Once ζ has been found for at least two peaks the proportional damping coefficients, α and β can be found from the following formulas:

$$\alpha = -2\frac{\omega_1\omega_2(\omega_1\zeta_2\sqrt{1-\zeta_2^2} - \omega_2\zeta_1\sqrt{1-\zeta_1^2})}{-\omega_1^2 + \omega_1^2\zeta_2^2 - \omega_2^2\zeta_1^2 + \omega_2^2} \tag{3}$$

$$\beta = \frac{-\alpha + \alpha\zeta_2^2 + 2\zeta_2\sqrt{1-\zeta_2^2}\,\omega_2}{\omega_2^2} \tag{4}$$

Using these formulas the following data was extracted from the frequency response data.

Table 1. Frequency response parameters from modal analysis and the MATLAB® model

Peak	Magnitude	Frequency	Coherence	ζ	MATLAB®
	dB (g/lbf)	Hz			Hz
1	-47.5769	19.25	0.9996	0.1542	19.29
2	-40.0984	64.25	0.9998	0.0471	63.36
3	-35.3801	123.50	0.9994		122.77
4	-36.8466	207.00	0.9980		205.85
α (s-1)	37.724				
β (s)	1.899E-6				

Comparing the experimental values with those from the MATLAB® model we see that there is good agreement between the two. Given that the resolution of the analyzer is 0.25 Hz we can say that the first mode is found exactly. The other modes are off by about 1 Hz. In the higher modes the system is found to actually be slightly stiffer than predicted. This is possibly due to the less than ideal boundary conditions. The calculated α and β are used in all the future models.

5. MATLAB® MODEL WITH VIBRATION ABSORBER

Now that the model has been validated for the plain barrel it must be modified to include the vibration absorber. As mentioned earlier the absorber is a proof mass type actuator that connects to the forward thermal shroud. The assembly consists of a shortened forward thermal shroud, onto which mounts the spring collar, onto which mount the leaf springs, which are in turn supported by the wedge collar. The shroud is 2.472 m in length and has a mass of 21 kg. The collar has a mass of 15.8 kg and has spaces for mounting up to eight springs. The leaf springs are trapezoidal in shape and 86 mm in length. The wedge collar screws onto the barrel threads for the standard thermal shroud. Its purpose is to preload the springs evenly. The springs should never loose contact with the wedge ring during normal operation.

Though up to eight springs can be used at once, only one was used in the model and during testing. This spring was mounted in the top location. Springs of three different spring constants were used in both the model and experiment. The three different spring types had thicknesses of 2, 2.8, and 3 mm, and spring constants, as ordered, of 87563, 204898, and 262690 N/m respectively. However these spring constants were for the springs under normal leaf spring type use conditions. With our setup this is not the case, so we installed each spring type, applied known weights and measured the deflection to get an apparent spring constant for our model. The measured spring constants for the 2, 2.8, and 3 mm springs were 175127, 269426, and 318412 N/m respectively.

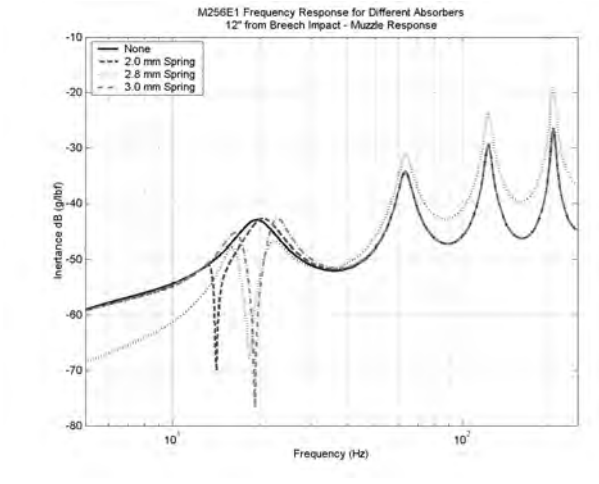

Figure 8 Predicted frequency response of the different absorbers

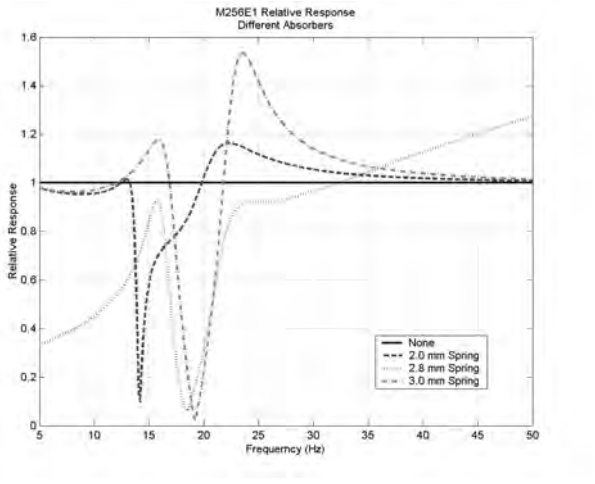

Figure 9 Relative frequency response of the different absorbers

The shroud was treated as a spring and thus by the standard approximation for a spring with mass, 1/3 of its mass was added to the absorber mass and 2/3 was added to the barrel as a lumped mass. The location of the lumped mass was adjusted so as that the center of gravity of the shroud and absorber mass together was positioned as in the actual assembly.

Table 2 Peak location versus spring type

Peak	None	2.0 mm	2.8 mm	3.0 mm
	Hz	Hz	Hz	Hz
A		13.83	16.24	16.90
1	19.29	20.28	21.51	22.47
2	63.36	63.38	63.40	63.41
3	122.77	122.76	122.76	122.76
4	205.85	205.86	205.86	205.86

The MATLAB® model allows for a mass and stiffness to be entered for a vibration absorber. The mass was a combination of the absorber mass and 1/3 of the shroud mass. These masses were removed from the non-beam mass part of the model so as that they wouldn't be counted twice. A separate model was made for each spring type. The stiffnesses found above were entered for the corresponding model. The resulting natural frequencies for each spring type were 13.92, 17.27, and 18.77 Hz for the 2, 2.8, and 3 mm models.

As with the plain barrel, the models were run once all required data was entered. Damped mode shapes and natural frequencies were recovered along with bode plots and pole-zero maps. Figure 8 shows the predicted frequency responses of the different absorbers in terms of the inertance. (Inertance is the ratio of vibration acceleration to force as a function of frequency[1].) Figure 9 shows the relative response of each absorber as compared to the original configuration. Whenever the trace is below the 1.0 line the response is less than the base system. If it is above the 1.0 line then the response is greater.

From Figure 8 the effects of the different absorbers on the first mode are readily apparent. The absorber is removing the first peak of the barrel and shifting its energy into new peaks on either side of it, as expected[9]. It can also be seen from the two plots that the absorber only affects the peak nearest it. The second and later peaks are not affected to any real degree. This is really noticeable in the relative response where the responses quickly return to a value of one after the first mode. At present we are not sure why the trace for the 2.8 mm spring does not follow this trend. Since it appears to be evenly offset from the rest of the traces we feel it is a coding error but have not been able to find it. Table 2 summarizes the locations of the modes for each of the absorbers. Peak A is the new peak created by the absorber.

6. VIBRATION ABSORBER TESTING

Now that we have a model including the vibration absorber, modal analyses were done to validate the model. The absorber was tested with each of the different spring types. The barrel orientation and accelerometer placement was kept the same as the last plain barrel test. This ensured that any changes in the frequency response should be directly attributable to the vibration absorber and not changes in test setup. The same procedure mentioned previously was

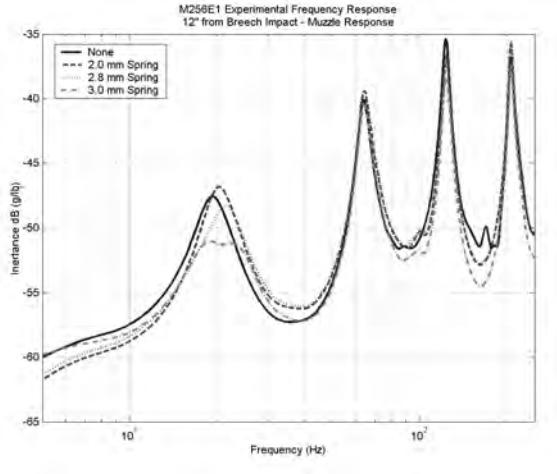

Figure 10 Frequency response of the different absorbers

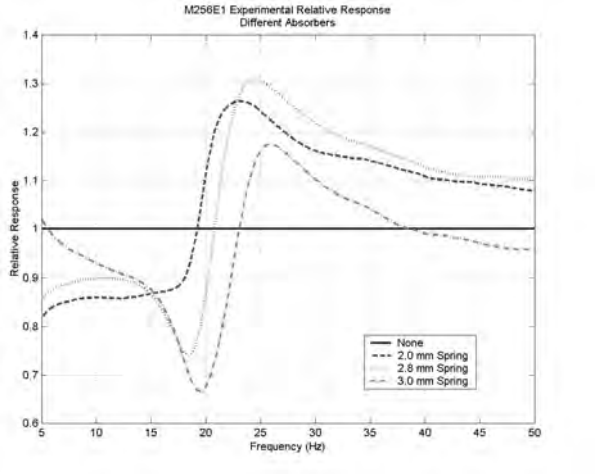

Figure 11 Relative frequency response of the different absorbers

followed for the tests.

The recovered frequency responses in terms of inertance are shown in Figure 10. Figure 11 shows the relative response of the absorbers as compared to the non-absorber system. Comparing these figures back to Figure 8 and Figure 9 some things are immediately apparent. First the expected notch for the absorber is missing from the 2.0 and 2.8 mm configurations. There is a slight notch on the 3.0 mm version. Graphically the shifting of the barrel's first peak and the lack of influence on the higher modes is still apparent though.

Table 3 Frequency response parameters from vibration absorber testing

No Vibration Absorber			
Peak	Magnitude	Frequency	Coherence
	dB (g/lbf)	Hz	
1	-47.5769	19.25	0.9996
2	-40.0984	64.25	0.9998
3	-35.3801	123.50	0.9994
4	-36.8466	207.00	0.9980
2.0 mm Vibration Absorber			
Peak	Magnitude	Frequency	Coherence
	dB (g/lbf)	Hz	
0			
1	-46.8353	20.25	0.9994
2	-39.4098	64.50	0.9993
3	-36.6398	124.00	0.9988
4	-35.7683	206.75	0.9985
2.8 mm Vibration Absorber			
Peak	Magnitude	Frequency	Coherence
	dB (g/lbf)	Hz	
0			
1	-48.3360	21.50	0.9998
2	-39.3727	64.50	0.9998
3	-36.8174	123.75	0.9994
4	-35.5993	207.00	0.9988
3.0 mm Vibration Absorber			
Peak	Magnitude	Frequency	Coherence
	dB (g/lbf)	Hz	
0	-51.0460	18.750	0.9988
1	-51.1914	22.50	0.9994
2	-40.5158	64.50	0.9996
3	-38.2738	123.75	0.9992
4	-37.3748	206.75	0.9992

Table 3 lists the frequency response parameters recovered from the experimental data. The data for the non-absorber configuration is repeated here to make comparisons easier. The same observations that can be made from comparing the graphs are just as apparent by comparing Table 2 and Table 3. Let's look at each of the configurations in individually.

The 2.0 mm absorber is missing the expected notch. From the MATLAB® model the notch should be at 13.83 Hz, however Figure 10 shows nothing at that frequency. The location of the next peak though matches between model and experiment. Both show it being shifted from 19.3 Hz to 20.3 Hz. They also show the absorber's effects being only noticeable around the first mode of the non-absorber barrel.

The 2.8 mm absorber shows the same trends as the 2.0 mm absorber. It too is missing the absorber notch and lower peak, this time it should be at 16.24 Hz. Peak 1 though once again matches between the model and experiment. Also the effects of the absorber are again localized around the effected mode, as they should be. Neither the 2.0 mm or the 2.8 mm absorber though appears to have any effect on the magnitude of the response around barrel's fist mode, as would be expected.

The 3.0 mm absorber tells a slightly different story though. This time the notch is there. It is small but it is detectable. The lower peak is at 18.75 Hz, which doesn't match with the model but is the calculated natural frequency of the absorber. The next peak does match with expectations. Over the frequency range between these two peaks the response is reduced by about 4 dB, which is noticeable though smaller than one would desire. Like the other two configurations the absorber's effects drop off quickly as one moves away from affected mode.

The lack of a notch for the absorbers is puzzling. They are having an effect on the barrel's mode near their natural frequencies by pushing it to a higher frequency but only the 3.0 mm one is having a noticeable effect on the magnitude. We are not sure what is causing this behavior. One idea we have come up with is that we are not getting enough energy into the system through the impact hammer. Without enough energy the friction and other nonlinearities in the components coupling the DTS to the system may not be overcome and thus it would not function properly. If this were correct this would be a lab only type problem, as getting energy into the system would not be a problem in test vehicle.

7. CONCLUSION

This paper has explored the effect of mounting a vibration absorber to the forward thermal shroud of a 120 mm M256E1 cannon. A MATLAB® model of the non-absorber barrel was developed and then verified by performing modal impact testing upon the actual barrel with the absorber rigidly affixed. Good agreement was found between the model and experimental data.

After modeling and testing the non-absorber barrel a vibration absorber was modeled and tested to find its effects upon the barrels frequency response. Three different configurations were modeled and tested. Decent agreement on the location of the modes was found between model and experiment. However the notch type effect of the absorber was missing from two of the three configurations. In the third it was noticeable but small. Only this third version attenuated the system response to any degree.

No explanation for this lack of absorber notch is readily apparent and verifiable. One possible one is that not enough energy is getting into the system through the impact hammer to overcome the friction and other nonlinearities in the components coupling the DTS to the system. At present though we have no plans on testing this theory, as there is no funding for more testing. The original version of the DTS though was tested on a vehicle and had no problems with getting enough energy into the system. If future testing of the DTS or similar devices is undertaken steps will be taken to make sure more energy can be gotten into the system. If done in the lab then most likely we will order a shaker or a change in boundary constraints. For testing in a vehicle getting energy into the system has never been a problem.

ACKNOWLEDGEMENTS

The authors would like to acknowledge the following individuals for their help in conducting this work: Kenneth Olsen, Paul Weber, Franz-Peter Speckert, Michael Gully, Gary Cunningham, and David Smith.

REFERENCES

1 Ewins, D. J., "*Modal Testing: Theory, Practice and Application*," Research Studies Press, Ltd., Baldock, England, 2000.
2 Kathe, E., "Gun Barrel Vibration Absorber," U.S. Patent 6167794, January 2001
3 Kathe, E., "MATLAB® Modeling of Non-Uniform Beams Using the Finite Element Method for Dynamics Design and Analysis," *U.S. Army ARDEC Report, ARCCB-TR-96010*, Benét Laboratories, Watervliet, NY, April 1996.
4 Kathe, E., "Lessons learned on the application of vibration absorbers for enhanced cannon stabilization," *Shock and Vibration*, **Vol. 8**, pp. 131 - 139, 2001.
5 Kathe, E. L., "Performance Assessment of a Synergistic Gun Barrel Vibration Absorber During Bump-Course Testing," *ARDEC Technical report ARCCB-TR-97022*, Benet Laboratories, Watervliet, NY, September 1997
6 Kathe, E., "Muzzle Break Vibration Absorber," U.S. Patent Application Serial Number 09/898.376, filed 5 July 2001.
7 Littlefield, A., Kathe, E., Messier, R., Olsen, K., "Gun Barrel Vibration Absorber to Increase Accuracy," *Proceedings of the 42nd AIAA/ASME/ASCE/AHS/ASC Structures, Structural Dynamics, and Materials Conference*, Seattle, WA 16 – 19 Apr 2001.
8 Kathe, E., "Design and Validation of a Gun Barrel Vibration Absorber" *Proceedings of the 67th Shock and Vibration Symposium*, Vol. 1, Published by SAVIAC, Monterey, CA, 18-22 November 1996, pp. 447-456.
9 Den Hartog, J. P., "*Mechanical Vibrations*," McGraw-Hill Book Company, Inc., New York, 1956.